

# RSC Advances



This is an *Accepted Manuscript*, which has been through the Royal Society of Chemistry peer review process and has been accepted for publication.

*Accepted Manuscripts* are published online shortly after acceptance, before technical editing, formatting and proof reading. Using this free service, authors can make their results available to the community, in citable form, before we publish the edited article. This *Accepted Manuscript* will be replaced by the edited, formatted and paginated article as soon as this is available.

You can find more information about *Accepted Manuscripts* in the [Information for Authors](#).

Please note that technical editing may introduce minor changes to the text and/or graphics, which may alter content. The journal's standard [Terms & Conditions](#) and the [Ethical guidelines](#) still apply. In no event shall the Royal Society of Chemistry be held responsible for any errors or omissions in this *Accepted Manuscript* or any consequences arising from the use of any information it contains.

Computational Study on Redox-Switchable Second-Order Nonlinear  
Optical Properties of Ferrocene-Tetrathiafulvalene Hybrid

Chun-Guang Liu<sup>†, ‡</sup>, Ming-Li Gao<sup>‡</sup>, and Zhi-Jian Wu<sup>\*†</sup>

<sup>†</sup> *State Key Laboratory of Rare Earth Resource Utilization, Changchun*

*Institute of Applied Chemistry, Chinese Academy of Sciences, Changchun City,*

*130022, P. R. China*

<sup>‡</sup> *College of Chemical Engineering, Northeast Dianli University Jilin City, 132012, P.*

*R. China*

### Abstract

Redox-switchable second-order nonlinear optical (NLO) responses of a series of ferrocene-tetrathiafulvalene (Fc-TTF) hybrids have been studied based on density functional theory calculations. The hyper-Rayleigh scattering (HRS) responses as well as the dynamic ( $\lambda = 1064$  nm) HRS hyperpolarizabilities have been calculated in gas phase within the T convention. The electron-correlation effects have been investigated. The long-range corrected LC-BLYP and wB97X-D functionals provide satisfactory results. The electron donor strength of the Fc-TTF in a donor- $\pi$ -conjugated-acceptor

---

\* Corresponding author.

E-mail addresses: zjwu@ciac.ac.cn

Tel.: 86-431-85262035. Fax: 86-431-85698041.

Present Addresses

No. 5625, Renmin Road, Changchun City, P. R. China.

structure has been assessed. The results indicate that the Fc unit does not display the role of the electron donor in the Fc-TTF unit. Because the Fc-TTF hybrid unit is a multistep redox center, the one- and two-electron-oxidized processes have been considered to control their second-order NLO responses. For a known Fc-TTF hybrid, the one-electron-oxidization leads to a significant increase of the HRS hyperpolarizability, while the calculated HRS hyperpolarizabilities are not affected by the two-electron-oxidization according to our DFT calculations. Interestingly, in another system the two-electron-oxidization significantly enhances the HRS hyperpolarizability, and the one-electron-oxidization does not largely affected the HRS hyperpolarizability.

## 1. Introduction

Because of the appealing potential applications in optical communication or data storage, the development of materials exhibiting switchable nonlinear optical (NLO) properties have motivated a number of works during the past two decades.<sup>1-3</sup> The reported method for switching of NLO properties includes redox,<sup>4-9</sup> protonation/deprotonation,<sup>10-12</sup> photoisomerization,<sup>13, 14</sup> boron site reduction,<sup>15</sup> ion induction in solution,<sup>16, 17</sup> etc. In order to obtain an effective redox-switching of second-order NLO responses (the molecular first hyperpolarizability  $\beta$ ), several questions should be considered. Such as, the stability of two forms relative to the switching of 'on' and 'off' is important because they can preferably be switched from one to other in an easily controlled way and the fast response time.<sup>7</sup> Molecular system with redox-switchable NLO responses is particularly attractive because the oxidation or reduction (removal or addition of electrons) enables fine control of their NLO properties. Although a large variety of redox-active molecular systems have been reported, the excellent redox center possessing the ability of reversible modification of second-order NLO responses is rare.

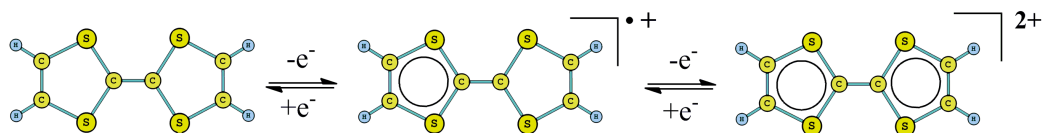


**Chart 1.** Sequential and reversible oxidization of TTF unit

As illustrated in Chart 1, the redox-active tetrathiafulvalene (TTF) unit is able to exist in three different stable redox states (TTF, the radical cation  $\text{TTF}^{\bullet+}$ , and dication  $\text{TTF}^{2+}$ ), and the oxidation to the radical cation and dication occurs sequentially and

reversibly at low potentials.<sup>18-24</sup> Due to the 14  $\pi$ -electron structure, the TTF unit is lack of a  $\pi$ -electron cyclic conjugation, and thus is nonaromatic according to Hückel rule. But the radical cation and dication with one and two 6  $\pi$ -electrons are aromatic in the Hückel sense, and thus both oxidized species are the thermodynamically stable. On the basis of the present points, the TTF unit is an ideal model for the redox switching of NLO responses. A series of redox-switchable second-order NLO molecules containing TTF unit have been studied experimentally and theoretically.<sup>13,14,25-27</sup> A large contrast in their second-order NLO responses has been obtained in TTF $\rightarrow$ TTF<sup>+</sup> oxidation. By contrast, the TTF<sup>+</sup> $\rightarrow$ TTF<sup>2+</sup> oxidation does not largely affect their second-order NLO responses.<sup>13,14</sup> It is well-known that the neutral TTF unit possesses a bent geometry, and the bent TTF unit changes to a fully planar geometry in the one-electron-oxidized process. Thus the large contrast in second-order NLO responses in TTF $\rightarrow$ TTF<sup>+</sup> oxidation is relative to a significant geometrical change of the TTF unit.

The ferrocene (Fc) is another typical redox center for reversibly modifying second-order NLO responses because it is easy to prepare and energetically convenient Fe<sup>II</sup>/Fe<sup>III</sup> couple.<sup>28-36</sup> It has been demonstrated that the oxidization of Fe<sup>II</sup> to Fe<sup>III</sup> caused the electron absorption spectra (charge transfer transition) of the Fe<sup>II</sup> and Fe<sup>III</sup> derivatives are decisively different from each other in a chromophore containing octamethylferrocenyl and nitro-thiophenyl groups.<sup>37</sup> According to sum-over-state description, any modification of the absorption spectrum of a molecule would alter the first hyperpolarizability. The hyper-Rayleigh scattering (HRS)

experiments indicated that the  $\text{Fe}^{\text{II}} \rightarrow \text{Fe}^{\text{III}}$  oxidization led to the first hyperpolarizability to decrease very substantially.

Due to the coexistence of 3d and  $\pi$ -spin electrons in the same molecule, the preparation of Fc-TTF hybrid has attracted considerable attention in the past three decades.<sup>38-46</sup> Several Fc-TTF and Fc-metalladithiolene hybrids have been reported, and their multistep redox properties have been investigated by cyclic voltammetry. However, their redox-switchable second-order NLO properties have not been explored. The molecule existing in two stable states to switching of second-order NLO response has been regarded as a good candidate for binary digital architecture because the redox interconversion between the two stable states matched the binary zero and one. In order to obtain a smaller molecule-based information-processing device component, the higher-order digit representation (such as ternary, senary, etc.) may be much superiority relative to binary.<sup>47</sup> Toward such goals, molecule must be able to exist in more than two stable and independently addressable states.<sup>48</sup> The Fc-TTF hybrid with multistep redox properties provides a very good basis for development of device component with high-order digit representation.

Here, we report a detailed theoretical study on a series of Fc-TTF hybrids with the aim of optimization of second-order NLO property by an effective combination of the Fc and TTF unit in the same molecule and describing the relationship between multistep redox properties and second-order NLO properties.

## 2. Computational details

All calculations were performed using Gaussian09 program.<sup>49</sup> The molecular structures were optimized and characterized as energy minima at B3LYP<sup>50-52</sup>/6-31g (d) level (LANL2DZ basis sets<sup>53-55</sup> for metal atom). The frequency-dependent hyperpolarizability was calculated by using time-dependent Hatree Fock (TDHF) and TD density functional theory (DFT) method at 1064 nm in this work.<sup>56-60</sup> The reliability of DFT with conventional XC functionals to evaluate the molecular hyperpolarizability has been questioned in a large number of studies. A correct description of the asymptotic behavior of the XC potential may be a prerequisite for the correct description of the first hyperpolarizability. Castet and Champagne have assessed a series of DFT XC functionals for evaluating the multipolar contributions to the first hyperpolarizability (the HRS responses) of some reference molecules.<sup>61</sup> They concluded that the best functionals were LC-BLYP,<sup>62</sup> M05-2X,<sup>63,64</sup> and M06-2X<sup>65</sup> for description of the HRS hyperpolarizability of their reference molecules. In the present paper, the six different functionals including BHandHLPY,<sup>66</sup> wB97X-D,<sup>67,68</sup> CAM-B3LYP<sup>69</sup>, LC-BLYP, M05-2X, and M06-2X have been employed to calculate the frequency-dependent hyperpolarizability. In order to evaluate the electron correlation effect of these functionals, as a reference the Hatree Fock (HF) method without electron-correlation consideration also has been carried out to calculate the frequency-dependent hyperpolarizability in this work. The basis sets containing diffuse and polarization functions are necessary for accurate predictions of hyperpolarizability according to many literatures. In the present paper, the 6-31+g(d)

basis sets with a good compromise between accuracy and computational costs for large molecular system have been employed for the first hyperpolarizability calculations (LANL2DZ basis sets for metal atom).

The available technology for measuring second-order NLO response is mainly HRS and electric field induced second harmonic generation (EFISHG) experimentally. HRS is the only experimental method to allow measuring the second-order NLO response of the charged species. Thus, we focused the HRS response in this work. Theoretically, Champagne et al. developed an effective method to estimate the HRS responses.<sup>70-77</sup> According to Bersohn's expression, the second-order NLO response  $\beta_{\text{HRS}}(-2\omega; \omega, \omega)$  can be extracted from HRS data by using the following equation:<sup>78, 79</sup>

$$\beta_{\text{HRS}}(-2\omega; \omega, \omega) = \sqrt{\langle \beta_{\text{ZZZ}}^2 \rangle + \langle \beta_{\text{XZZ}}^2 \rangle} \quad (1)$$

The depolarization ratio (DR), which is associated with the shape of the NLO-phore, given by

$$DR = \frac{\langle \beta_{\text{ZZZ}}^2 \rangle}{\langle \beta_{\text{XZZ}}^2 \rangle} \quad (2)$$

$\langle \beta_{\text{ZZZ}}^2 \rangle$  and  $\langle \beta_{\text{XZZ}}^2 \rangle$  are orientational averages of the  $\beta$  tensor, which were calculated without assuming Kleiman's conditions.<sup>80, 81</sup> All reported HRS hyperpolarizabilities are given in au (1 a.u. =  $3.6213 \times 10^{-42} \text{ m}^4 \text{ V}^{-1} = 8.639 \times 10^{-33} \text{ esu}$ ) within the T convention<sup>82</sup> as defined in ref. 82.

In order to get more insights of the origin of second-order NLO responses, the TDDFT method has been employed to calculate the nature of excited state. The excited energy, oscillator strengths, and associated major contributions of the orbital transitions for the studied molecule were determined at the B3LYP level using

6-31g(d) basis sets (LANL2DZ basis sets for metal atom). TDDFT is a usefully accurate approach for many applications,<sup>83</sup> especially, low-lying single excitations.

### 3. Results and discussion

#### 3.1. The donor strength of Fc-TTF hybrid

The typical second-order NLO chromophores have mostly focused on the donor- $\pi$  conjugated-acceptor (D- $\pi$ -A) structure. The Fc and TTF units are both the electron donor groups. The donor strength of the Fc unit is only comparable to the organic methoxyphenyl group according to experimental and theoretical studies.<sup>36</sup> And the donor strength of the TTF unit is slightly smaller than that of the typical N, N-bis-(4-methoxyphenyl)phenyl-amino donor based on our previous works.<sup>13</sup> However, the donor strength of the combination of Fc and TTF units has not been reported and is thus worthy of exploration. Firstly, an array model of the two donor groups in a same molecule should be considered. Several patterns of covalently bonded Fc and TTF units have been reported. Recently, a novel Fc-TTF hybrid, FcS<sub>4</sub>TTF(R)<sub>2</sub> (R = CF<sub>3</sub> and SMe (**H**)) (see Fig. 1), has been synthesized successfully, where the Fc and TTF units are linked to each other through an multisulfur  $\pi$ -conjugated bridge.<sup>84</sup> This compound is unique for designing the second-order NLO molecular system because the  $\pi$ -conjugated bridge would improve the coupling between the Fc and TTF units, and thus enhance their second-order NLO responses.

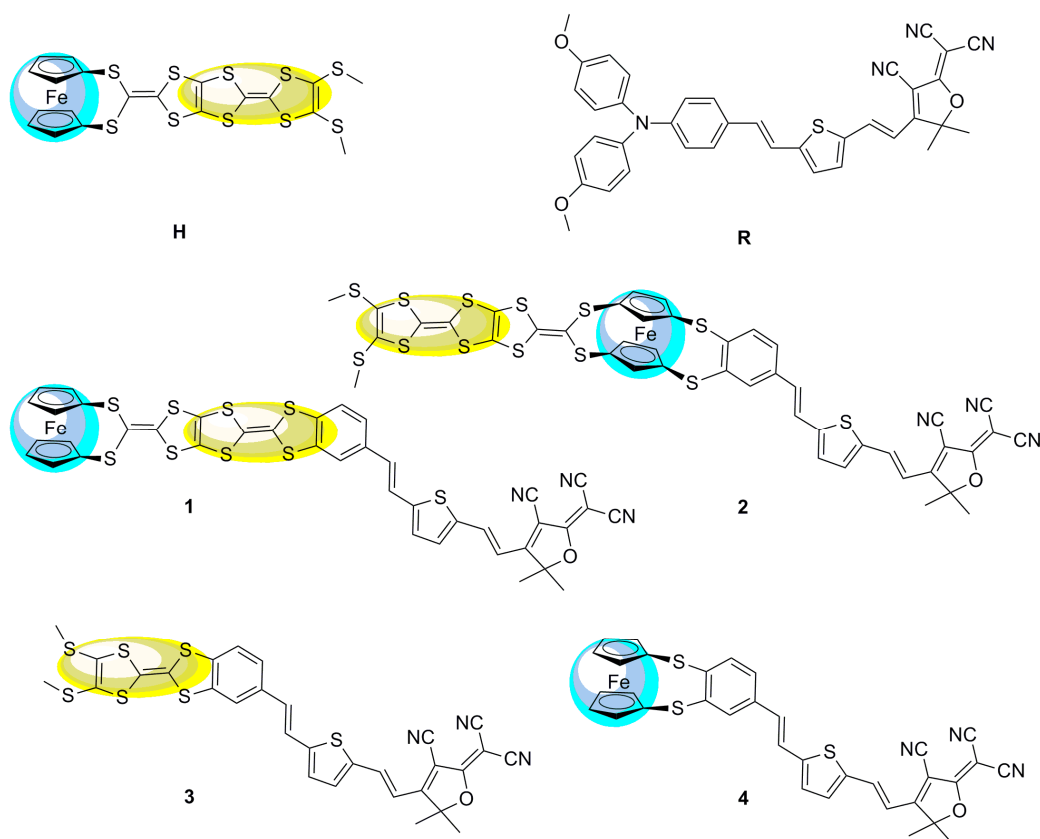


**Fig. 1** Structural formula of the Fc-TTF hybrid **H**, reference system **R**, and their derivatives **1**, **2**, **3**, and **4** (The yellow and blue color highlight TTF and Fc unit, respectively)

Due to the Fc and TTF units are both the electron donor, we will introduce a  $\pi$ -conjugated bridge and an electron acceptor to design a new molecular system with D- $\pi$ -A structure. A compound containing the key N, N-bis-(4-methoxyphenyl)phenyl-amino donor, 2, 5-divinylthienyl  $\pi$ -conjugated bridge, and the 2-dicyanomethylen-3-cyano-4-methyl-5-phenyl-5-trifluoromethyl-2,5-dihydrofuran acceptor (**R**) (see Fig. 1) has been chosen for designing the D- $\pi$ -A structure because the second-order NLO property of this compound has been investigated detailedly and broadly.<sup>85</sup> It has been demonstrated that this compound has

a 2-fold improvement in the molecular first hyperpolarizability and 3-fold macroscopic response than the simple triphenylamino analogue.<sup>86</sup>

**Table 1.** HRS first hyperpolarizability at 1064 nm in a.u.<sup>a</sup>. within the T convention

Compounds	Method	$\beta_{\text{HRS}}$	$\beta_{\text{HRS(DFT)}}/\beta_{\text{HRS(HF)}}$	DR
<b>H</b>	HF	80	—	4.97
	LC-BLYP	148	1.85	2.64
	wB97X-D	190	2.38	2.18
	CAM-B3LYP	177	2.21	2.16
	BHandHLYP	112	1.40	1.59
	M05-2X	213	2.66	2.26
	M06-2X	248	3.10	3.08
<b>1</b>	HF	77088	—	4.95
	LC-BLYP	119182	1.54	4.99
	wB97X-D	371371	4.81	5.00
	CAM-B3LYP	1609449	20.88	5.00
	BHandHLYP	65901109	852.93	5.01
	M05-2X	21752336	282.17	5.00
	M06-2X	3097211	40.09	5.00
<b>2</b>	HF	47448	—	4.91
	LC-BLYP	69202	1.46	4.98
	wB97X-D	137184	2.89	5.00
	CAM-B3LYP	208214	4.39	5.00
	BHandHLYP	215506	4.54	5.00
	M05-2X	201306	4.24	5.00
	M06-2X	229712	4.84	5.00
<b>3</b>	HF	77679	—	4.95
	LC-BLYP	121826	1.57	4.99
	wB97X-D	423339	5.45	5.00
	CAM-B3LYP	3608947	46.46	5.00
	BHandHLYP	3021202	38.89	5.00
	M05-2X	2328114	29.97	5.00
	M06-2X	1457492	18.76	5.00
<b>4</b>	HF	52042	—	4.91
	LC-BLYP	77112	1.48	4.97
	wB97X-D	159483	3.06	4.99
	CAM-B3LYP	253183	4.86	5.00
	BHandHLYP	203016	3.90	5.00
	M05-2X	246775	4.74	5.00
	M06-2X	288005	5.53	5.00

<sup>a</sup>1 a.u. =  $3.62 \times 10^{-42} \text{ m}^4 \text{ V}^{-1} = 8.64 \times 10^{-33} \text{ esu}$

As shown in Fig. 1, the donor moiety of **R** (N, N-bis-(4-methoxyphenyl)phenyl-amino) has been replaced with the Fc-TTF group (FcS<sub>4</sub>TTF(SMe)<sub>2</sub>), and thus we have systems **1** and **2**, where the  $\pi$ -A moiety of **R** was attached to the Fc-TTF group at TTF (**1**) and Fc (**2**) end, respectively. The frequency-dependent hyperpolarizabilities  $\beta_{\text{HRS}}(-2\omega; \omega, \omega)$  of **H**, **1**, and **2** have been calculated at HF, LC-BLYP, wB97X-D, CAM-B3LYP, BHandHLYP, M05-2X, and M06-2X levels using 6-31+g(d) basis sets (LANL2DZ basis sets for metal atom) in this work. The calculated  $\beta_{\text{HRS}}(-2\omega; \omega, \omega)$  values are given in Table 1. In order to estimate the electron correlation effects of different functionals, the ratio between the DFT-derived  $\beta_{\text{HRS}}(-2\omega; \omega, \omega)$  values and the corresponding HF values also has been reported in Table 1. It can be found that the  $\beta_{\text{HRS}}(\text{DFT})/\beta_{\text{HRS}}(\text{HF})$  ratio depends on the functional and differs from one molecule to another. Compared to the HF reference, all DFT calculations lead to an increase of the  $\beta_{\text{HRS}}(-2\omega; \omega, \omega)$  values for all three compounds. For **H** and **2**, the  $\beta_{\text{HRS}}(\text{DFT})/\beta_{\text{HRS}}(\text{HF})$  ratio is controlled in a reasonable range, where the ratio ranges from 1.40 to 3.10 in **H** and 1.46 to 4.84 in **2**. However, a significant difference is obtained in the case of **1**, where the fluctuation of  $\beta_{\text{HRS}}(\text{DFT})/\beta_{\text{HRS}}(\text{HF})$  ratio is very large (ranging from 1.54 to 852.93). This result confirms that the electron correlation effects of four functionals (CAM-B3LYP, BHandHLYP, M05-2X, and M06-2X) fail to describe the first hyperpolarizability because of a large fluctuation of  $\beta_{\text{HRS}}(\text{DFT})/\beta_{\text{HRS}}(\text{HF})$  ratio along with one molecule to another. By contrast, two functionals LC-BLYP and wB97X-D provide a rational result for the first hyperpolarizability calculation of **1**, where the  $\beta_{\text{HRS}}(\text{DFT})/\beta_{\text{HRS}}(\text{HF})$

ratio is 1.54 and 4.81, respectively. Especially the LC-BLYP functional, the calculated  $\beta_{\text{HRS}}(\text{DFT})/\beta_{\text{HRS}}(\text{HF})$  ratios of **H**, **1**, and **2** are in a narrow range (1.85 for **H**, 1.54 for **1**, and 1.46 for **2**). This result indicates that the major part of electron correlation effects is included at the LC-BLYP level for the three systems.

All the first hyperpolarizability calculations supported that (i) introduction of the  $\pi$ -A moiety into the studied molecular system leads to a substantial enhancement of the  $\beta_{\text{HRS}}(-2\omega;\omega,\omega)$  value (**1** vs **H** or **2** vs **H**); (ii) the second-order NLO responses are sensitive to the link location between D and  $\pi$ -A moieties (**1** vs **2**), where the system **1** (the  $\pi$ -A moiety of **R** was attached to the Fc-TTF group at TTF end) possesses the largest first hyperpolarizability among the three compounds. According to LC-BLYP calculation, the  $\beta_{\text{HRS}}(-2\omega;\omega,\omega)$  value of **1** is about 2 and 800 times as large as that of **2** and **H**, respectively. (iii) The DR increases to the 5 due to introduction of the  $\pi$ -A moiety, which demonstrates the NLO-phore of **1** and **2** would display ideal one-dimensional structures.

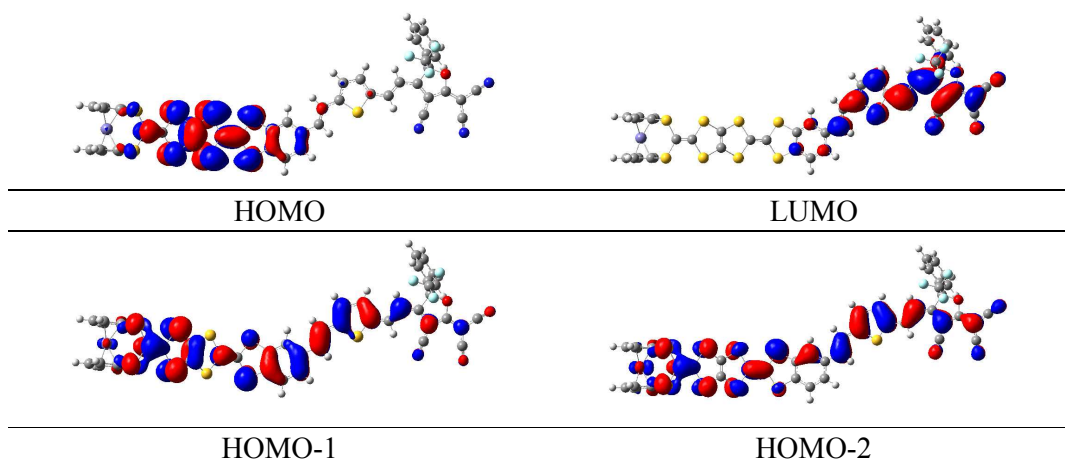
On the basis of the complex sum-over-states expression, Oudar and Chemla<sup>87, 88</sup> established a simple link between the molecular hyperpolarizability and a low-lying energy charge transfer transition through the two-level model,

$$\beta \propto (\mu_{ee} - \mu_{gg}) \frac{f_{os}}{\Delta E_{ge}^3}, \quad (3)$$

where  $\mu_{gg}$  and  $\mu_{ee}$  are the ground and excited state dipole moments,  $f_{os}$  is the oscillator strength, and  $\Delta E_{ge}$  is the transition energy. Those factors ( $\mu_{ee}-\mu_{gg}$ ,  $\Delta E_{ge}$  and  $f_{os}$ ) are all intimately related, and are controlled by electron properties of the donor/acceptor and the nature of the conjugated bridge.

**Table 2.** TDDFT-derived excited energy ( $E$ ), oscillator strength ( $f_{os}$ ), and major orbital transition for the system **1**

Compound	Excited state	$f_{os}$	$E$ (eV)	Major contributions
<b>1</b>	3	1.97	2.38	HOMO-1→LUMO(45%) HOMO→LUMO(24%) HOMO-2→LUMO(24%)



The TDDFT method has been carried out to calculate the excited state of the system **1**. The TDDFT calculated excited energy, oscillator strength, and associated orbital transition of the crucial excited state have been listed in Table 2. The crucial excited state is defined as the lowest optically allowed excited state with substantial oscillator strength. Our TDDFT calculations show that the crucial excited state of the system **1** is the third excited state. It contains the HOMO-1→LUMO (45%), HOMO→LUMO (24%), and HOMO-2→LUMO (24%) orbital transitions (see Table 2). The associated frontier molecular orbitals (FMOs) of the crucial excited state also have been listed in Table 2. It can be found that the HOMO is mainly localized on the TTF unit, and the LUMO is mainly localized on the electron acceptor end, which indicates that both FMOs are separated completely. This result indicates that the

HOMO→LUMO orbital transition would give a significant charge transfer (CT) from TTF unit to the electron acceptor end. However, due to the hardly any overlap between the two orbitals, such electron transition does not largely contribute to the crucial excited state (24%). By contrast, the major contribution arises from the HOMO-1→LUMO orbital transition (45%) according to our TDDFT calculations. As shown in Table 2, the HOMO-1 is delocalized over the whole molecule, combination of the electron distribution in the LUMO, which indicates that the crucial excitation of the system **1** can be viewed as a CT transition from the TTF unit to electron acceptor end. We also note that electron density on the Fc unit is very small in the series of occupied molecular orbitals (HOMO, HOMO-1, and HOMO-2). This indicates that the Fc unit does not display the role of electron donor in the system **1**.

In order to evaluate the donor strength of the Fc-TTF unit in the system **1** further, two new molecular systems **3** and **4** also have been considered in this work. Where each system only includes Fc or TTF donor (see Fig. 1). The frequency-dependent hyperpolarizabilities  $\beta_{\text{HRS}}(-2\omega;\omega,\omega)$  of **3** and **4** also have been calculated at the same levels, and are given in Table 1. As expected, all DFT calculations overestimate frequency-dependent hyperpolarizability  $\beta_{\text{HRS}}(-2\omega;\omega,\omega)$  value of both systems with respect to the HF reference. For the system **3**, the LC-BLYP and wb97X-D functionals satisfactorily describes the  $\beta_{\text{HRS}}(-2\omega;\omega,\omega)$  value, while CAM-B3LYP, BHandHLYP, M05-2X, and M06-2X functionals are failed again because of the overestimate of  $\beta_{\text{HRS}}(-2\omega;\omega,\omega)$  value with respect to the HF reference. For the system **4**, all the DFT calculations provide the  $\beta_{\text{HRS}}(\text{DFT})/\beta_{\text{HRS}}(\text{HF})$  ratio ranging from the

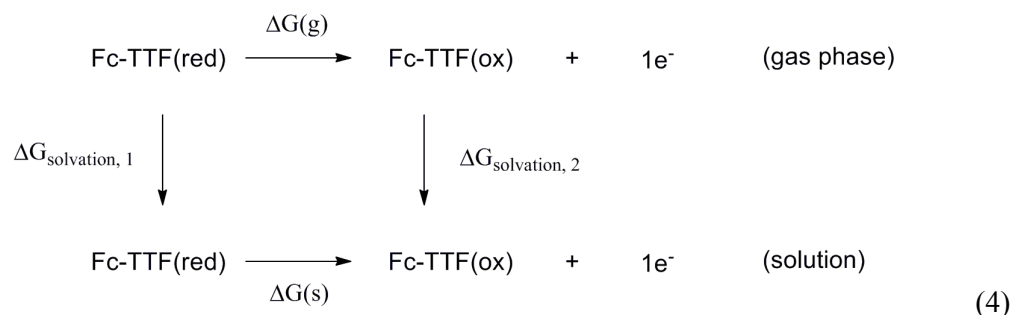
1.48 to the 5.53. Within the series of functionals considered in this study, the best functional for describing the second-order NLO response of the five systems appears to be LC-BLYP functional because of a stable  $\beta_{\text{HRS(DFT)}}/\beta_{\text{HRS(HF)}}$  ratio from one molecule to another (1.85 for **H**, 1.54 for **1**, 1.46 for **2**, 1.57 for **3**, and 1.48 for **4**). The wB97X-D functional also provide a well result with a  $\beta_{\text{HRS(DFT)}}/\beta_{\text{HRS(HF)}}$  ratio ranging from 2.35 to 5.45 along with the series of systems.

The LC-BLYP-derived  $\beta_{\text{HRS}(-2\omega;\omega,\omega)}$  values for **1** and **3** are 119182 and 121826 a.u., respectively. It is clearly show that the second-order NLO responses of **1** and **3** are very similar to each other. This result indicates that the second-order NLO properties of both systems are not sensitive to the presence of Fc unit (see Fig. 1). The Fc unit does not display the role of electron donor in the system **1**, which agrees well with the TDDFT calculations.

### 3.2. Redox-switchable second-order NLO response

The electrochemical properties of **H** have been reported. Cyclic voltammetry showed a series of reversible oxidation waves.<sup>84</sup> The first redox potential  $E_1^{\text{o/ox}}$  is at 0.11 V vs  $\text{Fc}^+/\text{Fc}$  (-0.33 V vs normal hydrogen electrode (NHE)), the second redox potential  $E_2^{\text{o/ox}}$  appears at 0.30 V vs  $\text{Fc}^+/\text{Fc}$  (-0.14 V vs NHE). And the first and second oxidation center of **H** has been assigned to the TTF and Fc moieties, respectively. We now estimate the cyclic voltammetric data of **H** based on the present DFT calculation. The theoretical estimation of the redox potential of a given molecular system requires determination of the free energy change of the

half-reactions, which is represented by the following thermodynamic cycle



The  $\Delta G(g)$  term represents the free energy associated with the oxidation of **H** in the gas phase; the next terms  $\Delta G_{\text{solvation}, 1}$  and  $\Delta G_{\text{solvation}, 2}$  correspond to the solvation free energies of the reduced and oxidized forms. Finally  $\Delta G(s)$  term is the free energy of the oxidation process in solution. The molecular geometries of **H** and its one- and two-electron-oxidized ( ${}^2\mathbf{H}^+_{\text{oxidized}}$  and  $\mathbf{H}^{2+}_{\text{oxidized}}$ ) species have been optimized at B3LYP/6-31g(d) levels in this work (LANL2DZ basis sets for metal atom). On the basis of the optimized geometries, the free energies of the species corresponding to the thermodynamic cycle have been calculated at the same level. The solvation free energies have been taken into account via the self-consistent reaction field (SCRF) method, using the integral equation formalism polarizable continuum model (IEFPCM) solvent model.<sup>89</sup> The SMD solvation model<sup>90</sup> proposed by Truhlar and coworkers has been performed for computing solvation free energies. A dielectric constant of acetonitrile has been employed in this work.

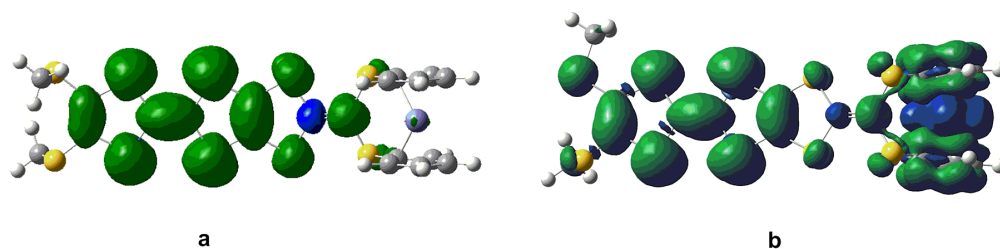


**Fig. 2** Spin density distribution of **H** in one- (a) and two-electron-oxidized species (b)

The Fe atom in **H** is formally in an oxidation state of +2 without unpaired d electrons, giving rise to a ground state with closed-shell configuration (singlet state). Due to removal of an electron from the singlet state, the spin state of the one-electron-oxidized species of **H** is doublet (an unpaired electron  ${}^2\mathbf{H}^+_{\text{oxidized}}$ ). The spin density distribution of  ${}^2\mathbf{H}^+_{\text{oxidized}}$  has been listed in Fig. 2. It can be found that the unpaired electron of  ${}^2\mathbf{H}^+_{\text{oxidized}}$  is mainly localized on the TTF moiety. This indicates that the first oxidation should take place preferentially at the TTF moiety. For the two-electron-oxidized species, the measurement of magnetic property showed that it possessed a diradical character with 3d and  $\pi$  spin.<sup>84</sup> And thus the optimized calculations have been carried out based on the broken-symmetry DFT method in this work. Meanwhile, the singlet state of the two-electron-oxidized species ( ${}^1\mathbf{H}^{2+}_{\text{oxidized}}$ ) also has been considered. Our DFT calculations show that the most stable species is the antiferromagnetic state ( ${}^{\text{anti}}\mathbf{H}^{2+}_{\text{oxidized}}$ ). The calculated total energy including the electronic and zero-point corrected energies of  ${}^{\text{anti}}\mathbf{H}^{2+}_{\text{oxidized}}$  is  $\sim 82.32$  kJ mol<sup>-1</sup> stable than  ${}^1\mathbf{H}^{2+}_{\text{oxidized}}$ . As shown in Fig. 2, the spin densities of  ${}^{\text{anti}}\mathbf{H}^{2+}_{\text{oxidized}}$  are mainly localized over the Fe center and TTF moiety with antiferromagnetic spin alignment (blue,  $\alpha$  spin; green,  $\beta$  spin). Combined with the spin density of  ${}^2\mathbf{H}^+_{\text{oxidized}}$ , all results indicate that the second oxidized center should be the Fe center. Taking into account

all the above points, our DFT calculations well reproduced the oxidation center of **H** when compared with the experimental studies.

On the basis of the ground-state structure for the series of oxidized species of **H**, we will reproduce the redox potential of the present studies Fc-TTF hybrid. The half-reaction of normal hydrogen electrode (NHE) is defined as  $1/2\text{H}_2(\text{g}) \rightarrow \text{H}^+(\text{aq}) + \text{e}^-(\text{g})$ , and the absolute reduction potential of the NHE has been computed to be 4.36 eV (Note that the sign of the absolute potential depends on the direction in which the reaction is written: the absolute oxidation potential of the hydrogen electrode is negative while the absolute reduction potential is positive).<sup>91</sup> Using this value and these oxidation potentials, the free energies of the two oxidation processes are consequently estimated to be -4.71 and -4.48 V according to experimental studies.<sup>84</sup> Our DFT calculated energies is -4.70 and -4.49 V, which is well in agreement with the experimental values.

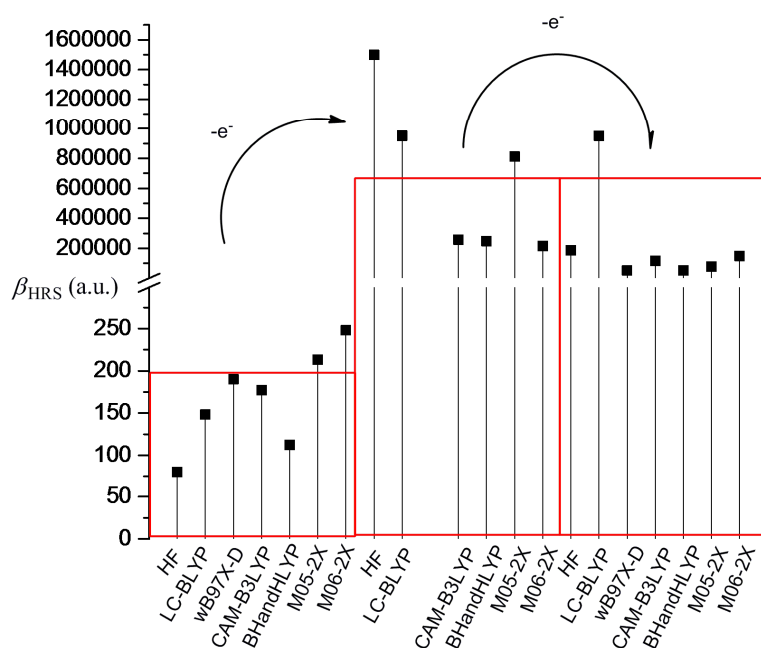


**Fig. 3** Comparisons of the frequency-dependent first hyperpolarizability of **H** in different redox states (The wB97X-D-derived  $\beta_{\text{HRS}}(-2\omega;\omega,\omega)$  value of the one-electron-oxidized species has not been achieved because of the bad SCF convergence)

The frequency-dependent hyperpolarizability of  ${}^2\text{H}^+$  oxidized and  $\text{anti-}\text{H}^{2+}$  oxidized also has been calculated at HF, LC-BLYP, wB97X-D, CAM-B3LYP, BHandHLYP, M05-2X, and M06-2X levels using 6-31+g(d) basis sets (LANL2DZ basis sets for metal atom) in this work. The calculated  $\beta_{\text{HRS}}(-2\omega;\omega,\omega)$  values are compared in Fig. 3. It can be found that a substantial enhancement of the second-order NLO response has been obtained in one-electron-oxidized process, while the second-order NLO response has no change after two-electron oxidation. As mentioned above, the one-electron-oxidized center of **H** is TTF unit. This indicates that one-electron oxidation will affect the geometrical structure of the TTF unit. The crystallographic

study and our DFT calculations both show that the TTF unit in neutral **H** forms a bent structure, while the bent TTF unit changes to a planar structure after one-electron oxidation. Due to the two-electron-oxidized center is the Fc unit, the TTF unit is still planar after two-electron oxidation. This result shows that the first hyperpolarizability is sensitive to the structural transformation of the TTF unit in the series of oxidized processes. The planar TTF unit with the well conjugated feature will enhance the second-order NLO response.

**Table 3.** TDDFT-derived excited energy ( $\Delta E$ ), oscillator strength ( $f_{os}$ ), and major orbital transition for the system **H** and its one- and two-electron-oxidized species

Compounds	$f_{os}$	$\Delta E$ (eV)	Major Contributions
<b>H</b>	0.21	3.96	HOMO→LUMO+6 (+41%) HOMO→LUMO+9(+22%)
<sup>2</sup> <b>H</b> <sup>+</sup> <sub>oxidized</sub>	0.34	0.96	$\beta$ HOMO→ $\beta$ LUMO(100%)
<sup>anti</sup> <b>H</b> <sup>2+</sup> <sub>oxidied</sub>	0.26	1.29	HOMO→LUMO(100%)

The TDDFT calculated excited energy and oscillator strength of the crucial excited state for **H**, <sup>2</sup>**H**<sup>+</sup><sub>oxidized</sub> and <sup>anti</sup>**H**<sup>2+</sup><sub>oxidied</sub> has been listed in Table 3. It can be found that calculated oscillator strength of the three species is on the same order. The one-electron-oxidized process leads to a 4-fold decrease of the excited energy, where it decreases from 3.96 to 0.96 eV. By contrast, the two-electron-oxidized process does not largely affect the magnitude of the excited energy. The calculated excited energy changes from 0.96 to 1.29 eV. According to the two-level model, the decrease of excited energy would enhance the second-order NLO properties, which is in agreement with the hyperpolarizability calculation.

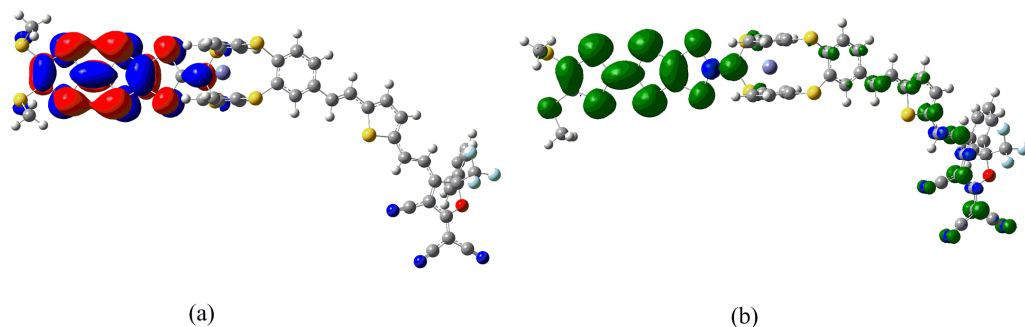


**Fig. 4** The HOMO of **2** (a) and the spin density distribution of its one-electron-oxidized species  ${}^2\mathbf{2}^+_{\text{oxidized}}$  (b)

In the purpose of improvement of the role of Fc unit in switching of second-order NLO response in the series of oxidized process, the system **2** may be a well candidate because the Fc unit acts as the role of a bridge between TTF unit and  $\pi$ -A moiety (see Fig. 1). It is well known that the redox property of molecule is closely associated with the nature of frontier molecular orbital. As shown in Fig. 4, the HOMO of **2** is mainly localized on the TTF unit. This indicates that the one-electron-oxidized center of **2** may be the TTF unit. Thus, unrestricted optimized calculations of one-electron-oxidized species  ${}^2\mathbf{2}^+_{\text{oxidized}}$  (the one-electronic-oxidized species has one unpaired electron, and thus a doublet state), are performed to check predictions made by molecular orbital analysis. It can be seen from Fig. 4 that the spin density of  ${}^2\mathbf{2}^+_{\text{oxidized}}$  mainly localizes on the exTTF unit, which is well in agreement with the molecular orbital predictions. For two-electron-oxidized species of  ${}^2\mathbf{2}^+_{\text{oxidized}}$ , two possible spin states (singlet and triplet state,  ${}^1\mathbf{2}^+_{\text{oxidized}}$  and  ${}^3\mathbf{2}^+_{\text{oxidized}}$ ) have been optimized at B3LYP/6-31g(d) level (LANL2DZ basis set on metal ion). The results indicate that the singlet state is 40.33 kJ/mol lower than the triplet state. The NBO charges of Fe(II) atom and TTF unit for **2**,  ${}^2\mathbf{2}^+_{\text{oxidized}}$  and  ${}^1\mathbf{2}^+_{\text{oxidized}}$  have been

calculated at B3LYP levels using 6-31g(d) basis sets (LANL2DZ basis set on metal ion), and have been listed in Table 4. It can be found that the calculated NBO charge of the TTF unit is positive and Fe(II) center is negative. The NBO charge of TTF unit gets a significantly increase in one- and two-electron-oxidized processes (0.18 for **2**, 0.49 for  ${}^2\mathbf{2}^+$ <sub>oxidized</sub>, and 1.54 for  ${}^1\mathbf{2}^{2+}$ <sub>oxidized</sub>). By contrast, the NBO charge of the Fe(II) center does not change largely in the series of oxidized processes. This result also supports that TTF unit is the oxidized center in the series of oxidized processes.

**Table 4.** HRS first hyperpolarizability at 1064 nm in a.u. within the T convention, the TDDFT-derived excited energy ( $\Delta E$ ) and oscillator strength ( $f_{os}$ ), and NBO charge ( $Q$ ) of TTF unit and Fe center for **2**,  ${}^2\mathbf{2}^+$ <sub>oxidized</sub>, and  ${}^1\mathbf{2}^{2+}$ <sub>oxidized</sub>

Compounds	Functionals	$\beta_{\text{HRS}}$	DR	$Q(\text{TTF})$	$Q(\text{Fe})$	$f_{os}$	$\Delta E$ (eV)
<b>2</b>	LC-BLYP	69202	4.98	0.18	-0.26	1.33	2.26
	CAM-B3LYP	208214	5.00				
	M05-2X	201306	5.00				
	M06-2X	229712	5.00				
${}^2\mathbf{2}^+$ <sub>oxidized</sub>	LC-BLYP	595922	5.15	0.49	-0.13	1.46	2.24
	CAM-B3LYP	71464	3.43				
	M05-2X	266744	1.59				
	M06-2X	71541	3.95				
${}^1\mathbf{2}^{2+}$ <sub>oxidized</sub>	LC-BLYP	142565526	2.06	1.54	-0.28	0.18	0.41
	CAM-B3LYP	924110	4.00				
	M05-2X	2888725	2.15				
	M06-2X	13657080	3.68				

$${}^a\text{1 a.u.} = 3.62 \times 10^{-42} \text{ m}^4 \text{ V}^{-1} = 8.64 \times 10^{-33} \text{ esu}$$

The frequency-dependent hyperpolarizability of  ${}^2\mathbf{2}^+$ <sub>oxidized</sub> and  ${}^1\mathbf{2}^{2+}$ <sub>oxidized</sub> has been calculated at LC-BLYP, CAM-B3LYP, M05-2X, and M06-2X levels using 6-31+g(d) basis sets (LANL2DZ basis sets for metal atom) in this work. The calculated  $\beta_{\text{HRS}}(-2\omega; \omega, \omega)$  values have been listed in Table 4. It can be found that the LC-BLYP functional gives the largest  $\beta_{\text{HRS}}(-2\omega; \omega, \omega)$  values for the one- and

two-electron-oxidized species and the smallest  $\beta_{\text{HRS}}(-2\omega;\omega,\omega)$  value for the neutral system **2** among all four functionals, and thus the LC-BLYP functional overestimates the redox-switchable effects on optical nonlinearity when compared with the CAM-B3LYP-, M05-2X-, and M05-2X-derived results. All four functionals show that the two-electron-oxidized process significantly enhances the second-order NLO property. Although the one-electron-oxidized process also leads to an enhancement of the  $\beta_{\text{HRS}}(-2\omega;\omega,\omega)$  value, this enhancement is weak relevant to the two-electron-oxidized process according to our DFT calculations. On the other hand, the DR values of  ${}^2\mathbf{2}^+_{\text{oxidized}}$  and  ${}^1\mathbf{2}^{2+}_{\text{oxidized}}$  are smaller than that of **2**, which indicates that the NLO-phore is off ideal one-dimensional structures.

The TDDFT calculated excited energy and oscillator strength of the crucial excited state for **2**,  ${}^2\mathbf{2}^+_{\text{oxidized}}$  and  ${}^1\mathbf{2}^{2+}_{\text{oxidized}}$  also has been listed in Table 4. The results indicate that the excited energy and oscillator strength are not sensitive to the one-electron-oxidized process, and are on the same order of magnitude for **2** and  ${}^2\mathbf{2}^+_{\text{oxidized}}$ . It is well-known that the first hyperpolarizability is inversely proportional to the cube of excited energy and proportional to the oscillator strength, the analogous magnitudes of excited energy and oscillator strength imply small change of the first hyperpolarizability (see Table 4). Thus it will lead to a small enhancement on the first hyperpolarizability in the one-electron-oxidized process. By contrast, the crucial excited energies of  ${}^1\mathbf{2}^{2+}_{\text{oxidized}}$  are significantly lower than that of **2** and  ${}^2\mathbf{2}^+_{\text{oxidized}}$ , the crucial excited energies of  ${}^1\mathbf{2}^{2+}_{\text{oxidized}}$  are  $\sim 5.6$  and  $\sim 5.3$  times as small as that of **2** and  ${}^2\mathbf{2}^+_{\text{oxidized}}$ , respectively. The very low excited energy will generate a substantial

increase in the second-order NLO responses, which is well in agreement with the hyperpolarizability calculations with all four functionals.

#### 4. Conclusions

In the present paper, the HF and various DFT XC functionals have been employed to evaluate the HRS responses of a series of Fc-TTF hybrids. The total HRS first hyperpolarizability,  $\beta_{\text{HRS}}(-2\omega;\omega,\omega)$ , has been calculated in gas phase within the T convention. The 6-31+g(d) basis sets containing diffuse and polarization functions have been used. The calculated HRS hyperpolarizabilities are dependent on the XC functionals: the long-range corrected LC-BLYP and wB97X-D functionals provide good performances on the computed  $\beta_{\text{HRS}}(-2\omega;\omega,\omega)$  values of the series of Fc-TTF hybrids.

The donor strength of the Fc-TTF unit in the D- $\pi$ -A structure has been elucidated through the HRS hyperpolarizability and TDDFT calculations. We found that the calculated hyperpolarizability is not sensitive to the presence of Fc unit. And the electron density distributions on the Fc unit in the series of frontier molecular orbitals (HOMO, HOMO-1, and HOMO-2), which is associated with the crucial excited state, is nearly zero. All results indicate that Fc unit in the Fc-TTF hybrid does not display the role of electron donor. Duo to the Fc-TTF hybrid possesses a series of reversible oxidation waves, the redox-switchable second-order NLO responses of Fc-TTF hybrid have been explored based on our DFT calculations. The HRS hyperpolarizabilities here computed for the one- and two-electron-oxidization have been compared. The

calculated HRS hyperpolarizability are not affected in any significant way by the two-electron-oxidization. Differently, when going from the neutral Fc-TTF hybrid to the one-electron-oxidized species, the HRS hyperpolarizability remarkably increases. Interestingly, in another system the two-electron-oxidization significantly enhances the HRS hyperpolarizability, while HRS hyperpolarizability is not largely affected by the one-electron-oxidization.

### **Acknowledgments**

The authors gratefully acknowledge the financial support from the National Natural Science Foundation of China (21373043), Chinese Postdoctoral Science Foundation (2013M540261), and the Scientific Research Foundation for Doctor of Northeast Dianli University (BSJXM-201110).

### **SUPPLEMENTARY MATERIAL**

Xyz coordinates for all structures reported in this paper. This materials is available free of charge via the Internet at <http://pubs.rsc.org>.

### **References**

- 1 M. Albota, D. Beljonne, J. -L. Brédas, J. E. Ehrlich, J.-Y. Fu, A. A. Heikal, S. E. Hess, T. Kogej, M. D. Levin, S. R. Marder, D. McCored-Maughon, J. Perry, W. H. Rockel, M. Rumi, G. Subramaniam, W. W. Webb, X.-L. Wu, C. Xu, *Science*. 1998, **281**, 1653-1656.

- 2 Y. Shi, C. Zhang, H. Zhang, J. H. Bechtel, L. R. Dalton, B. H. Robinson, W. H. Steier, *Science*. 2000, **288**, 119-122.
- 3 M. Lee, H. E. Katz, C. Erben, D. M. Gill, P. Gopalan, J. D. Heber, D. J. McGee, *Science*. 2002, **298**, 1401-1403.
- 4 B. J. Coe, S. Houbrechts, I. Asselberghs, A. *Angew. Chem. Int. Ed.* 1999, **38**, 366-369.
- 5 B. J. Coe, *Acc. Chem. Res.* 2006, **39**, 383-393.
- 6 C. Sporer, I. Ratera, D. Ruiz-Molina, Y. Zhao, J. Vidal-Gancedo, K. Wurst, P. Jaitner, K. Clays, A. Persoons, C. Rovira, J. A. Veciana, *Angew. Chem. Int. Ed.* 2004, **43**, 5266-5268.
- 7 M. Malaun, Z. R. Reeves, R. L. Paul, J. C. Jeffery, J. A. McCleverty, M. D. Ward, I. Asselberghs, K. Clays, A. Persoons, *Chem. Commun.* 2001, **20**, 49-50.
- 8 K. A. Green, M. P. Cifuentes, M. Samoc, M. G. Humphrey, *Coord. Chem. Rev.* 2011, **255**, 2530-2541.
- 9 B. J. Coe, *Coord. Chem. Rev.* 2013, **257**, 1438-1458.
- 10 S. Muhammad, H. L. Xu, M. R. S. A. Janjua, Z. M. Su, M. Nadeem, *Phys. Chem. Chem. Phys.*, 2010, **12**, 4791-4799
- 11 F. Mancuois, L. Sanguinet, J.-L. Pozzo, M. Guillaume, B. Champagne, V. Rodriguez, F. Adamietz, L. Ducasse, F. Castet, *J. Phys. Chem. B* 2007, **111**, 9795-9802.
- 12 L. Sanguinet, J.-L. Pozzo, V. Rodriguez, F. Adamietz, F. Castet, L. Ducasse, B. Champagne, *J. Phys. Chem. B* 2005, **109**, 11139-11150.

- 13 C. G. Liu, Z. M. Su, X. H. Guan, S. Muhammad, *J. Phys. Chem. C* 2011, **115**, 23946–23954.
- 14 C. G. Liu, X. H. Guan, *Phys. Chem. Chem. Phys.* 2012, **14**, 5297-5306.
- 15 S. Muhammad, M. R. S. A. Janjua, Z. M. Su, *J. Phys. Chem. C* 2009, **113**, 12551–12557
- 16 S. Muhammad, T. Minani, H. Fukui, K. Yoneda, R. Kishi, Y. Shigeta, M. Nakano, *J. Phys. Chem. A* 2011, **116**, 1417-1424.
- 17 S. Muhammad, C. G. Liu, L. Zhao, S. X. Wu, Z. M. Su, *Theor. Chem. Account* 2009 **122**, 77–86.
- 18 J. Becher, J. O. Jeppesen, K. Nielsen, *Synth. Met.* 2003, **133–134**, 309-315.
- 19 J. O. Jeppesen, J. Becher, *Eur. J. Org. Chem.* 2003, **2003**, 3245-3266.
- 20 M. R. Bryce, *J. Mater. Chem.* 2000, **10**, 589-598.
- 21 J. L. Segura, N. Martín, *Angew. Chem. Int. Ed.* 2001, **40**, 1372-1409.
- 22 D. Canevet, M. Sallé, G. Zhang, D. Zhang, D. Zhu, *Chem. Commu.* 2009, **17**, 2245-2269.
- 23 M. B. Nielsen, C. Lomholt, J. Becher, *Chem. Soc. Rev.* 2000, **29**, 153-164.
- 24 J. F. Lamère, I. Malfant, A. Sournia-Saquet, P. G. Lacroix, *Chem. Mater.* 2007, **19**, 805-815.
- 25 C. G. Liu, W. Guan, P. Song, L. K. Yan, Z. M. Su, *Inorg. Chem.* 2009, **48**, 6548-6554.
- 26 C. G. Liu, X. H. Guan, Z. M. Su, *J. Phys. Chem. C* 2011, **115**, 6024–6032.
- 27 C. G. Liu, *Mol. Phys.* 2014, **112**, 199-205.

- 28 G. Guirado, C. Coudret, J.-P. Jaunay, *J. Phys. Chem. C*. 2007, **111**, 2770–2776.
- 29 B. J. Coe, R. J. Docherty, S. P. Foxon, E. C. Harper, M. Helliwell, J. Raftery, K. Clays, E. Franz, B. S. Brunshwig, *Organometallics*. 2009, **28**, 6880–6892.
- 30 Y. Liao, B. E. Eichinger, K. A. Firestone, M. Haller, J. Luo, W. Kaminsky, J. B. Benedict, P. J. Reid, A. K-Y. Jen, L. R. Dalton, B. H. Robinson, *J. Am. Chem. Soc.* 2005, **127**, 2758–2766.
- 31 A. Trujillo, M. Fuentealba, D. Carrillo, C. Manzur, I. Ledoux-Pak, J.-R. Hamon, J.-Y. Saillard, *Inorg. Chem.* 2010, **49**, 2750–2764.
- 32 G. Li, Y. Song, H. Hou, L. Li, Y. Fan, Y. Zhu, X. Meng, L. Mi, *Inorg. Chem.* 2003, **42**, 913–920.
- 33 T. L. Kinnibrugh, S. Salman, Y. A. Getmanenko, V. Coropceanu, III, W. W. Porter, T. V. Timofeeva, A. J. Matzger, J.-L. Brédas, S. R. Marder, S. Barlow, *Organometallics*. 2009, **28**, 1350–1357.
- 34 B. J. Coe, J. Fielder, S. P. Foxon, I. Asselberghs, K. Clays, B. S. Van Cleuvenbergen, *Organometallics*. 2011, **30**, 5731–5743.
- 35 H. K. Sharma, K. H. Pannell, I. Ledoux, J. Zyss, A. Ceccanti, P. Zanello, *Organometallics*. 2000, **19**, 770–774.
- 36 S. D. Bella, *Chem. Soc. Rev.* 2001, **30**, 355–366.
- 37 M. Malaun, Z. R. Reeves, R. L. Paul, J. C. Jeffery, J. A. McCleverty, M. D. Ward, I. Asselberghs, K. A. Clays, *Chem. Commun.* 2001, 49–50.
- 38 A. J. Moore, P. J. Skabara, M. R. Bryce, A. S. Batsanov, J. A. K. Howard, S. T. A. K. Daley, *J. Chem. Soc. Chem. Commun.* 1993, **4**, 417–419.

- 39 S. B. Wilkes, I. R. Butler, A. E. Underhill, A. Kobayashi, H. Kobayashi, *J. Chem. Soc. Chem. Commun.* 1994, **1**, 53–54.
- 40 S. B. Wilkes, I. R. Butler, A. E. Underhill, M. B. Hursthouse, D. E. Hibbs, K. M. A. Malik, *J. Chem. Soc. Dalton Trans.* 1995, **7**, 897–903.
- 41 H.-J. Lee, D.-Y. Noh, A. E. Underhill,; C.-S. Lee, *J. Mater. Chem.* 1999, **9**, 2359–2363. (h) P. J. Skabara, M. R. Bryce, A. S. Batsanov, J. A. K. Howard, *J. Org. Chem.* 1995, **60**, 4644–4646.
- 42 R. Andreu, J. Garin, J. Orduna, M. Saviron, S. Uriel, *Synth. Met.* 1995, **70**, 1113–1114.
- 43 H.-J. Lee,; D.-Y. Noh, *J. Mater. Chem.* 2000, **10**, 2167–2172.
- 44 M. Iyoda, T. Takano, N. Otani, K. Ugawa, M. Yoshida, H. Matsuyama, Y. Kuwatani, *Chem. Lett.* 2001, **30**, 1310–1311.
- 45 U. T. Mueller-Westerhoff, R. W. Sanders, *Organometallics.* 2003, **22**, 4778–4782.
- 46 T. Kusamoto, K. Takada, R. Sakamoto, S. Kume, H. Nishihara, *Inorg. Chem.* 2012, **51**, 12102–12113.
- 47 K. A. Green, M. P. Cifuentes, T. C. Corkery, M. Samoc, M. G. Humphrey, *Angew. Chem. Int. Ed.* 2009, **48**, 7867–7870.
- 48 K. Szacilowski, *Chem. Rev.* 2008, **108**, 3481–3548.
- 49 M. J. Frisch, G. W. Trucks, H. B. Schlegel, G. E. Scuseria, M. A. Robb, J. R. Cheeseman, G. Scalmani, V. Barone, B. Mennucci, G. A. Petersson, H. Nakatsuji, M. Caricato, X. Li, H. P. Hratchian, A. F. Izmaylov, J. Bloino, G. Zheng, J. L. Sonnenberg, M. Hada, M. Ehara, K. Toyota, R. Fukuda, J. Hasegawa, M. Ishida, T.

Nakajima, Y. Honda, O. Kitao, H. Nakai, T. Vreven, J. A. Montgomery, J. E. Peralta, F. Ogliaro, M. Bearpark, J. J. Heyd, E. Brothers, K. N. Kudin, V. N. Staroverov, R. Kobayashi, J. Normand, K. Raghavachari, A. Rendell, J. C. Burant, S. S. Iyengar, J. Tomasi, M. Cossi, N. Rega, J. M. Millam, M. Klene, J. E. Knox, J. B. Cross, V. Bakken, C. Adamo, J. Jaramillo, R. Gomperts, R. E. Stratmann, O. Yazyev, A. J. Austin, R. Cammi, C. Pomelli, J. W. Ochterski, R. L. Martin, K. Morokuma, V. G. Zakrzewski, G. A. Voth, P. Salvador, J. J. Dannenberg, S. Dapprich, A. D. Daniels, O. Farkas, J. B. Foresman, J. V. Ortiz, J. Cioslowski, D. J. Fox, Gaussian, Inc., Wallingford CT, 2009.

50 A. D. Becke, *J. Chem. Phys.* 1993, **98**, 5648-5652.

51 C. Lee, W. Yang, R. G. Parr, *Phys. Rev. B*, 1988, **37**, 785-789.

52 B. Miehlich, A. Savin, H. Stoll, H. Preuss, *Chem. Phys. Lett.* 1989, **157**, 200-206.

53 P. J. Hay, W. R. Wadt, *J. Chem. Phys.* 1985, **82**, 270-284.

54 W. R. Wadt, P. J. Hay, *J. Chem. Phys.* 1985, **82**, 284-299.

55 P. J. Hay, W. R. Wadt, *J. Chem. Phys.* 1985, **82**, 299-311.

56 J. Olsen, P. Jorgensen, *J. Chem. Phys.* 1985, **82**, 3235-3264.

57 H. Sekino, R. J. Bartlett, *J. Chem. Phys.* 1986, **85**, 976-989.

58 J. E. Rice, N. C. Handy, *J. Chem. Phys.* 1991, **94**, 4959-4971.

59 J. E. Rice, R. D. Amos, S. M. Colwell, N. C. Handy, J. Sanz, *J. Chem. Phys.* 1990, **93**, 8828-8839.

60 J. E. Rice, N. C. Handy, *Int. J. Quantum Chem.* 1992, **43**, 91-118.

61 F. Castet, B. Champagne, *J. Chem. Theory Comput.* 2012, **8**, 2044-2052.

- 62 H. Iikura, T. Tsuneda, T. Yanai, K. Hirao, *J. Chem. Phys.* 2001, **115**, 3540-3544.
- 63 Y. Zhao, N. E. Schultz, D. G. Truhlar, *J. Chem. Phys.* 2005, **123**, 1611031-1611034.
- 64 Y. Zhao, N. E. Schultz,; D. G. Truhlar, *J. Chem. Theory and Comput.* 2006, **2**, 364-382.
- 65 Y. Zhao, D. G. Truhlar, *Theor. Chem. Acc.* 2008, **120**, 215-241.
- 66 A. D. Becke, *J. Chem. Phys.* 1993, **98**, 1372-1377.
- 67 J.-D. Chai, M. Head-Gordon, *J. Chem. Phys.* 2008, **128**, 084106.
- 68 J.-D. Chai,; M. Head-Gordon, *Phys. Chem. Chem. Phys.* 2008, **10**, 6615-6620.
- 69 T. Yanai, D. Tew, N. Handy, *Chem. Phys. Lett.* 2004, **393**, 51-57.
- 70 M. Guillaume, B. Champagne, N. Markova, V. Enchev, F. Castet, *J. Phys. Chem. A.* 2007, **111**, 9914-9923.
- 71 F. Mançois, L. Sanguinet, J.-L. Pozzo, M. Guillaume, B. Champagne, V. Rodriguez, F. Adamietz, L. Ducasse, F. Castet, Acido-Triggered Nonlinear Optical Switches: Benzazolo-oxazolidines. *J. Phys. Chem. B.* 2007, **111**, 9795-9802.
- 72 A. Plaquet, M. Guillaume, B. Champagne, L. Rougier, F. Mançois, V. Rodriguez, J.-L. Pozzo, L. Ducasse, F. I. Castet, *J. Phys. Chem. C.* 2008, **112**, 5638-5645.
- 73 A. Plaquet, M. Guillaume, B. Champagne, F. Castet, L. Ducasse, J.-L. Pozzo, V. Rodriguez, *Phys. Chem. Chem. Phys.* 2008, **10**, 6223-6232.
- 74 F. Mançois, J.-L. Pozzo, J. Pan, F. Adamietz, V. Rodriguez, L. Ducasse, F. Castet, A. Plaquet, B. Champagne, *Chem. Eur. J.* 2009, **15**, 2560-2571.
- 75 E. Bogdan, L. Rougier, L. Ducasse, B. Champagne, F. Castet, *J. Phys. Chem.* 2010,

**114**, 8474-8479.

76 E. Bogdan, A. Plaquet, L. Antonov, V. Rodriguez, L. Ducasse, B. Champagne, F. Castet, *J. Phys. Chem.* 2010, **114**, 12760-12768.

77 B. Champagne, A. Plaquet, J.-L. Pozzo, V. Rodriguez, F. Castet, *J. Am. Chem. Soc.* 2012, **134**, 8101-8103.

78 R. Bersohn, Y. H. Pao, H. L. Frisch, *J. Chem. Phys.* 1966, **45**, 3184-3199.

79 F. Castet, E. Bogdan, A. Plaquet, L. Ducasse, B. Champagne, V. Rodriguez, *J. Chem. Phys.* 2012, **136**, 024506-024521.

80 D. Qi, NLO Calculator, version 0.2; University of Science and Technology Beijing: Beijing, China, 2012.

81 L. J. Zhang, D. D. Qi, L. Y. Zhao, C. Chen, Y. Z. Bian, W. J. Li, *J. Phys. Chem.* 2012, **116**, 10249-10256.

82 A. Willetts, J. E. Rice, D. M. Burland, D. P. Shelton, *J. Chem. Phys.* 1992, **97**, 7591-7599.

83 M. A. L. Marques, A. Rubio, *Phys. Chem. Chem. Phys.* 2009, **11**, 4436-4436.

84 T. Kusamoto, H. Nishihara, R. Kato, *Inorg. Chem.* 2013, **52**, 13809-13811.

85 L. R. Dalton, P. A. Sullivan, D. H. Bale, *Chem. Rev.* 2010, **110**, 25-55.

86 Y. J. Cheng, J. D. Luo, S. Hau, D. H. Bale, T. -D. Kim, Z. Shi, D. B. Lao, N. M. Tucker, Y. Tian, L. R. Dalton, P. J. Reid, A. K. Y. Jen, *Chem. Mater.* 2007, **19**, 1154-1163.

87 J. L. Oudar, D. S. Chemla, *J. Chem. Phys.* 1977, **66**, 2664-2668.

88 J. L. Oudar, *J. Chem. Phys.* 1977, **67**, 446-457.

- 89 J. Tomasi, B. Mennucci, R. Cammi, *Chem. Rev.* 2005, **105**, 2999-3094.
- 90 A. V. Marenich, C. J. Cramer, D. G. Truhlar, *J. Phys. Chem.* 2009, *113*, 6378-6396.
- 91 A. Lewis, J. A. Bumpus, D. G. Truhlar, C. J. Cramer, *J. Chem. Educ.* 2004, **81**, 596-604.